Genes & Diseases (2022) 9, 1674–1688

Available online at www.sciencedirect.com

ScienceDirect

journal homepage: http://ees.elsevier.com/gendis/default.asp

FULL LENGTH ARTICLE

# Discovery of a tetrahydroisoquinoline-based CDK9-cyclin T1 protein–protein interaction inhibitor as an anti-proliferative and anti-migration agent against triple-negative breast cancer cells

**Shasha Cheng [a,1], Guan-Jun Yang [a,1], Wanhe Wang [b,c,1], Dik-Lung Ma [b,**], Chung-Hang Leung [a,d,*]**

[a] *State Key Laboratory of Quality Research in Chinese Medicine, Institute of Chinese Medical Sciences, University of Macau, Taipa, Macao SAR, PR China*
[b] *Department of Chemistry, Hong Kong Baptist University, Kowloon Tong, Hong Kong SAR, PR China*
[c] *Institute of Medical Research, Northwestern Polytechnical University, Xi'an, Shaanxi 710072, PR China*
[d] *Department of Biomedical Sciences, Faculty of Health Sciences, University of Macau, Macao SAR, PR China*

Received 12 March 2021; received in revised form 31 May 2021; accepted 7 June 2021
Available online 10 July 2021

**KEYWORDS**
Cancer stem cells;
CDK9-cyclin T1;
Epithelial mesenchymal transition;
Protein–protein interaction (PPI);
Triple-negative breast cancer (TNBC)

**Abstract** Triple-negative breast cancer (TNBC) is a highly aggressive and metastasizing cancer that has the worst prognosis out of all breast cancer subtypes. The epithelial–mesenchymal transition (EMT) and cancer stem cells (CSCs) have been proposed as important mechanisms underlying TNBC metastasis. CDK9 is highly expressed in breast cancer, including TNBC, where it promotes EMT and induces cancer cell stemness. In this study, we have identified a tetrahydroisoquinoline derivative (compound **1**) as a potent and selective CDK9-cyclin T1 inhibitor via virtual screening. Interestingly, by targeting the ATP binding site, compound **1** not only inhibited CDK9 activity but also disrupted the CDK9-cyclin T1 protein–protein interaction (PPI). Mechanistically, compound **1** reversed EMT and reduced the ratio of CSCs by blocking the CDK9-cyclin T1 interaction, leading to reduced TNBC cell proliferation and migration. To date, compound **1** is the first reported tetrahydroisoquinoline-based CDK9-cyclin T1 ATP-competitive inhibitor that also interferes with the interaction between CDK9 and cyclin

* Corresponding author.
** Corresponding author.
*E-mail addresses:* edmondma@hkbu.edu.hk (D.-L. Ma), duncanleung@um.edu.mo (C.-H. Leung).
Peer review under responsibility of Chongqing Medical University.
[1] These authors contributed equally to this work.

https://doi.org/10.1016/j.gendis.2021.06.005

T1. Compound **1** may serve as a promising scaffold for developing more selective and potent anti-TNBC agents. Our work also provides insight into the role of the CDK9-cyclin T1 PPI on EMT and CSCs and highlights the feasibility and significance of targeting CDK9 for the treatment of TNBC.



## Introduction

Triple-negative breast cancer (TNBC) is a difficult cancer to treat due to its high rate of recurrence and metastasis.[1,2] The aggressive behavior of TNBC has been linked to cancer stem cells (CSCs) and the epithelial—mesenchymal transition (EMT).[3,4] CSCs represent a population of cells with high self-renewal and differentiation ability in primary tumors and metastases. In solid tumors, CD44 and CD133 are common CSC biomarkers, either used alone or in combination with CD24.[5] In breast cancer patients, bone marrow metastases and pleural metastases have high proportions of $CD44^{+}/CD24^{-}$ cells.[6] Meanwhile, EMT is a cellular process in which malignant epithelial cells modify their transcriptional expression to lose cell attachments and to become more motile and mesenchymal.[7] The EMT promotes the invasive and metastatic behavior of epithelial cancers.[8,9] The initiation of EMT requires the activity of transcription factors, such as Twist, Snail, and ZEB1/2.[10] In order to maintain the growth of metastatic lesions, a fraction of tumor cells have to retain CSC properties to sustain the proliferative reservoir.[10] The CSC phenotype is typically not inflexible but very dynamic, which has been associated with an intermediate EMT condition.[11] Hence, inhibiting CSCs and EMT could be an important strategy for the treatment of TNBC.

Cyclin-dependent kinase 9 (CDK9) is overexpressed in many types of human cancer, especially in TNBC.[12,13] As an important protein kinase among the CDK family, it plays key roles in maintaining basal gene transcription and thus transcriptional homeostasis.[14] CDK9 is paired with cyclin T1 to form the main part of the human positive transcription elongation factor b (P-TEFb) complex, which regulates cell proliferation and apoptosis.[15] Cyclin T1 is essential for maintaining CDK9 activity.[15] Mounting evidence indicates that CDK9 is a promising therapeutic target for human diseases, including TNBC.[16,17] The simultaneous inhibition of CDK9 and tumor stem cells has been shown to enhance antitumor activity.[18] Moreover, the inhibition of P-TEFb downregulates the expression of the EMT transcription factors Twist1 and Snail, and further delay tumor progression.[19] The expression of Snail is regulated by P-TEFb and its transcription can be activated by Twist1.[20] Targeting CDK9 to inhibit cancer stemness has also recently aroused interest and some CDK9 inhibitors have been designed to suppress EMT and CSCs for cancer treatment.[18] However, it is still unclear how CDK9 is responsible for mediating the underlying mechanism of EMT and CSCs. In particular, the further development of CDK9-cyclin T1 protein—protein interaction (PPI) modulators is urgently needed as chemical probes or potential anti-TNBC agents.

Natural products have been a major source of pharmaceutical molecules in history.[21] However, the limited supplies and structural complexity of natural products have presented challenges for scientists seeking to harness natural product scaffolds for medicine.[22—24] In this context, virtual screening can be a highly efficient and cost-effective strategy for identifying lead compounds from natural products. In this work, we report the discovery of a potent and selective small-molecule CDK9-cyclin T1 PPI inhibitor (compound **1**) from a natural product/natural product-like database using high-throughput virtual screening. Interestingly, in addition to inhibiting CDK9 kinase activity, compound **1** also blocked the PPI between CDK9 and cyclin T1. In TNBC cells, compound **1** decreased EMT and CSC biomarkers, resulting in potent anti-proliferative and anti-migration effects. Therefore, compound **1** is a promising lead structure for the future development of more effective drug leads against TNBC.

## Materials and methods

### Molecular modeling

A chemical library containing over 280,000 natural products or natural product-like compounds (ZINC natural product database) was used for docking. The initial model of CDK9-cyclin T1 in complex with A86 was constructed from the X-ray crystal structure (PDB: 6GZH) using the molecular conversion procedure implemented in the ICM-pro 3.6-1d program (Molsoft).[25] The molecular conversion and molecular docking procedures were performed as in previous reports.[22]

### Cells and reagents

Human embryonic kidney (HEK 293T) cells, normal liver (LO2) cells, normal breast (MCF-10A) cells and breast cancer (MDA-MB-231, MDA-MB-468, BT549, T47D) cell lines were cultured in DMEM (Gibco, CA, USA) supplemented with 1% penicillin and streptomycin, and 10% fetal bovine serum (Gibco). Cells were incubated at 37°C/5% $CO_2$ in a humidified atmosphere. Compounds **1**—**14** (purity $>$ 95%) were purchased from J&K Scientific Ltd. (Hong Kong, China). The positive control dinaciclib (**15**) was bought from Selleck (Houston, CA, USA). All the compounds were dissolved in dimethyl sulfoxide (DMSO). The CDK9 Assay Kit was obtained from BSP Bioscience (San Diego, CA, USA). Actinomycin D (ActD) and cycloheximide (CHX) were purchased from Beyotime (Shanghai, China). TurboFect™ Transfection

Reagent was purchased from Thermal Fisher (Catalog number: R0532). The sources of the antibodies are indicated separately in the procedures below. CD44-FITC and CD24-APC were purchased from BioLegend (San Diego, CA, USA). MTT (3-(4,5-dimethylthiazol-2-yl)-2,5-diphenyltetrazolium bromide) was obtained from Sigma—Aldrich (St. Louis, MO, USA).

## CDK9-cyclin T activity screening assay

The screening of CDK9-cyclin T PPI inhibitors was performed by a chemiluminescence assay following the manufacturer's instructions. Briefly, the master mixture (25 μL per well, containing 6 μL 5 × Kinase assay buffer + 1 μL ATP (500 μM) + 10 μL 5 × CDK substrate peptide + 8 μL distilled water) was prepared. Then, inhibitor solution (5 μL) was added into test wells and 20 μL of 1 × Kinase assay buffer was added to the control well. CDK9/cyclin T1 enzyme (20 μL) was assigned to the positive control and test wells and incubated at 30°C. After 45 min, the amounts of remaining ATP in the kinase reaction were quantified by Kinase-Glo using a SpectraMax M5 microplate reader (Molecular Devices, San Jose, CA, USA).

## Western blotting

MDA-MB-231 and MDA-MB-468 cells were seeded in a 6-well plate at a density of $1 \times 10^5$/mL and incubated overnight. The Western blot assay was performed as the previous report.[26] The antibodies against CDK9 (1:1000), Cyclin T1 (1:1000), and β-actin (1:1000) were purchased from Abcam (Cambridge, MA, USA). Twist1 (1:1000), Snail (1:1000), OCT4 (1; 1000), CD44 (1:1000), and CD133 (1:1000) were purchased from Absin Bioscience (Shanghai, China). Proteins bands were detected using enhanced chemiluminescent Plus reagents (GE Healthcare) and analyzed by Image Lab.

## Cellular thermal shift assay

MDA-MB-231 cells were seeded in a 100 $cm^2$ dish at a density of $1 \times 10^5$/mL. The cellular thermal shift assay was performed to detect the target engagement of compound **1** in MDA-MB-231 cell lysates as described in our previous report.[2]

## CDK9 knockdown assay

MDA-MB-231 cells were seeded in a 6-well plate and incubated at 80% confluence. Lipo3000 reagent, control scrambled siRNA (SC-35847, Santa Cruz Biotechnologies, Dallas, TX, USA), CDK9 siRNA 5′-GGAGAAUUUUACUGUGUUUtt-3′ were mixed with DMEM medium for 20 min at 37°C, before adding to cells. After 48 h post-transfection, the cell density was 95%.

## CDK9 plasmid transfection

The HA-CDK9 plasmid was purchased from Addgene (catalog: 28102). MDA-MB-231 cells were seeded in a 6-well plate at a density of $2 \times 10^5$ cell/mL. DMEM was mixed with empty vector control or HA-CDK9 plasmid combined with TurboFect for 15 min at 37°C, before adding to cells. Transgene expression was analyzed after 24—48 h.

## Cell cytotoxicity and proliferation assay

MDA-MB-231, MDA-MB-468, BT549, T47D, MCF-10A, LO2, and HEK293T cell cytotoxicity and proliferation were evaluated by MTT and colony formation assays as in our previous report.[27]

## Transwell assay

MDA-MB-231, MDA-MB-468, and MCF-10A cells were seeded in Transwell inserts ($1 \times 10^4$ cells/well). Migration ability was detected by the Transwell assay as in our previous report.[28]

## Co-immunoprecipitation (co-IP) assay

MDA-MB-231 cells were seeded in 75 $cm^2$ flask with density of $1 \times 10^5$/mL. Cells were incubated with indicated concentration of compound **1**, **15**, or DMSO for 12 h. Cell lysates were collected, and protein concentrations were determined using the Pierce BCA protein assay kit. 20 μg of each protein sample were incubated overnight with 10 μL pre-incubated anti-cyclin T1 magnetic beads based on manufacturer's protocol. Then, protein levels were analyzed by Western blotting.

## Chromatin immunoprecipitation assay

Chromatin immunoprecipitation (ChIP) assays were performed according to manufacturer's protocols (Millipore, Bedford, MA, USA) with slight modifications. MDA-MB-231 cells treated with compound **1** or **15** (5 μM) or DMSO control for 12 h and cross-linked by incubating with 1% (vol/vol) formaldehyde-containing medium for 10 min at 37°C. Then chromatin with DNA fragments between 200 and 1000 base pairs. Anti-CDK9 (Santa Cruz Biotechnology) and Anti-IgG (Cell Signaling Technology) was used to capture DNA fragments. Purification was performed using the ChIP DNA Purification Kit (Active Motif, Carlsbad, CA, USA). ChIP-PCR analysis were performed by real-time qPCR (ViiA™ 7 System, Life Technologies). The PCR primers for the target promoters are shown in Table S1.

## $CD44^+/CD24^-$ staining analysis

MDA-MB-231 cells were seeded in 100 $cm^2$ dish at a density of $1 \times 10^5$/mL, then treated with compound **1** or **15** (5 μM) or DMSO control for 12 h. Cells were collected and washed with PBS, followed by incubation for 30 min at 4°C with FITC- and APC-conjugated anti-mouse IgG or FITC-conjugated anti-CD44 and APC-conjugated anti-CD24

antibodies. Cells were analyzed by flow cytometry using a BD LSR Fortessa Flow Cytometer.

### Cell cycle analysis

MCF-10A, LO2, and MDA-MB-231 cells were seeded in 6-well plate at a density of $1 \times 10^5$/mL and incubated overnight. After treatment with 5.0 μM compound **1** or **15** for 12 h, cells were harvested and washed in cold PBS. Cells were fixed with 70% ethanol at −20°C overnight. Then, Cell Cycle and Apoptosis Analysis Kit (Beyotime, Shanghai, China) were used according to the manufacturer's instruction. Briefly, cells were incubated with RNase A and propidium iodide for 30 min at room temperature, and analyzed by flow cytometry using a BD LSR Fortessa Flow Cytometer.

### 3D cell sphere formation assay

MDA-MB-231 and MDA-MB-468 cells ($1 \times 10^3$/mL) were seeded in Nunclon™ Sphera™ Dishes (Thermo Fisher Scientific) cultured with DMEM/F12 medium, B27 (1:50, Gibco), human recombinant epidermal growth factor (20 ng/mL, Gibco), and basic fibroblast growth factor (20 ng/mL, Gibco). Cells were incubated with compound **1** (10 or 30 μM) or DMSO control for two weeks, and 3D cell spheres were observed using confocal laser scanning microscopy. The volume of spheres was quantified by Image J software.

### Statistical analysis

All statistical tests were performed using GraphPad Prism version 8.0 (Graph Pad, San Diego, CA, USA). Statistical significance was determined using the Student's *t*-test for experiments comparing two groups. Comparisons among groups were analyzed using analysis of variance (ANOVA). Unless stated otherwise, *P* values were 2-tailed and considered significant if $P < 0.05$. Error bars represent SEM of three experiments unless stated otherwise.

## Results

### Compound 1 is identified as a novel CDK9-cyclin T1 inhibitor via *in silico* screening

The high-resolution crystal structure of human CDK9-cyclin T1 in complex with A86, a CDK9-cyclin T1 activity inhibitor (PDB: 6GZH),[25] was used as a molecular model for virtual screening using the internal coordinate mechanics (ICM) method [ICM-Pro 3.6-1d program (Molsoft, San Diego, CA, USA)]. Against this structure, 280,000 natural product or natural product-like compounds (ZINC natural product database) were docked against the ATP-binding site. From the virtual screening results (Table 1), the top hit compounds **1**−**14** (Fig. 1) were tested by a CDK9-cyclin T1 chemiluminescence assay using the clinical CDK9 inhibitor dinaciclib (**15**) as a positive control (Fig. 2A). Compounds **1**, **2**, **3** and **6**, which showed greater than 60% inhibition activity in the initial screen, were tested in a dose−response experiment using chemiluminescence assay to further quantitate their inhibitory potency, revealing $IC_{50}$ values of 3.0, 3.9, 6.0, and 6.6 μM, respectively against CDK9-cyclin T1 kinase activity (Fig. 2B−E).

**Table 1** ZINC number and docking scores of compounds tested in this study.

| Name | ZINC No. | Relative molecular weight (Mr) | Scores (CDK9-cyclin T1) |
|---|---|---|---|
| 1 | ZINC20113732 | 438.480 | −36.1 |
| 2 | ZINC19703291 | 347.751 | −37.1 |
| 3 | ZINC00489528 | 339.728 | −37.1 |
| 4 | ZINC12296628 | 540.576 | −36.5 |
| 5 | ZINC08790017 | 452.396 | −34.9 |
| 6 | ZINC20756959 | 299.259 | −35.3 |
| 7 | ZINC06624166 | 383.400 | −36.1 |
| 8 | ZINC70691544 | 350.418 | −38.2 |
| 9 | ZINC06624559 | 383.536 | −35.1 |
| 10 | ZINC12296964 | 326.360 | −37.3 |
| 11 | ZINC96113717 | 493.488 | −40.59 |
| 12 | ZINC96114636 | 416.385 | −40.75 |
| 13 | ZINC96114889 | 432.384 | −40.88 |
| 14 | ZINC96116054 | 514.442 | −37.98 |

Compounds **1**, **2**, **3** and **6**, were brought forward for *in cellulo* testing. The EMT biomarker Twist1 is directly regulated by CDK9.[20] Therefore, Twist1 protein levels were detected to verify the potential biological effect of the compounds in TNBC cells. The results showed that compound **1** exhibited the greatest reduction of Twist1 expression in MDA-MB-231 cells (Fig. 2F). Moreover, a time course showed that compound **1** achieved optimal inhibition activity at 12 h (Fig. S1).

### Binding mode of compound 1 and kinetics analysis

Molecular modeling revealed the interaction between compound **1** and the CDK9-cyclin T1 complex. The docking results showed that compound **1** is situated in the CDK9-cyclin T1 ATP-binding pocket, forming two hydrogen bonds with the residues lining the binding site (Fig. 3A). Moreover, the hydroxyl group of compound **1** acts as an H-bonding acceptor with Glu66's side chain, which has been reported to contribute to the selectivity and potency of CDK9 inhibitors.[29] The imine group of compound **1** was also predicted to act as an H-bonding acceptor with Lys48. Interestingly, our docking analysis suggested that the predicted binding mode of compound **1** was very distinct to that calculated for ATP (Fig. 3B) or dinaciclib (**15**) (Fig. 3C). For example, compound **1** is not predicted to protrude as far into the binding cavity as ATP or **15**, hence the H-bonds formed between ATP and Asp104 and Cys106 and between **15** and Asp109 and Cys106 are not present in the binding model of compound **1**. Instead, compound **1** is situated closer to the other side of the site near the hinge region, forming H-bonds to Glu66 and Lys48 that are not present in the other two structures. We performed an enzyme kinetics assay to validate the binding mode of compound **1**. The results showed that compound **1** inhibited CDK9-cyclin T1 activity with a $K_i$ value of $2.14 \pm 0.2$ μM and was competitive with ATP (Fig. 3E, F). This result supports the hypothesis that **1** targets the ATP-binding site of CDK9-cyclin T1.

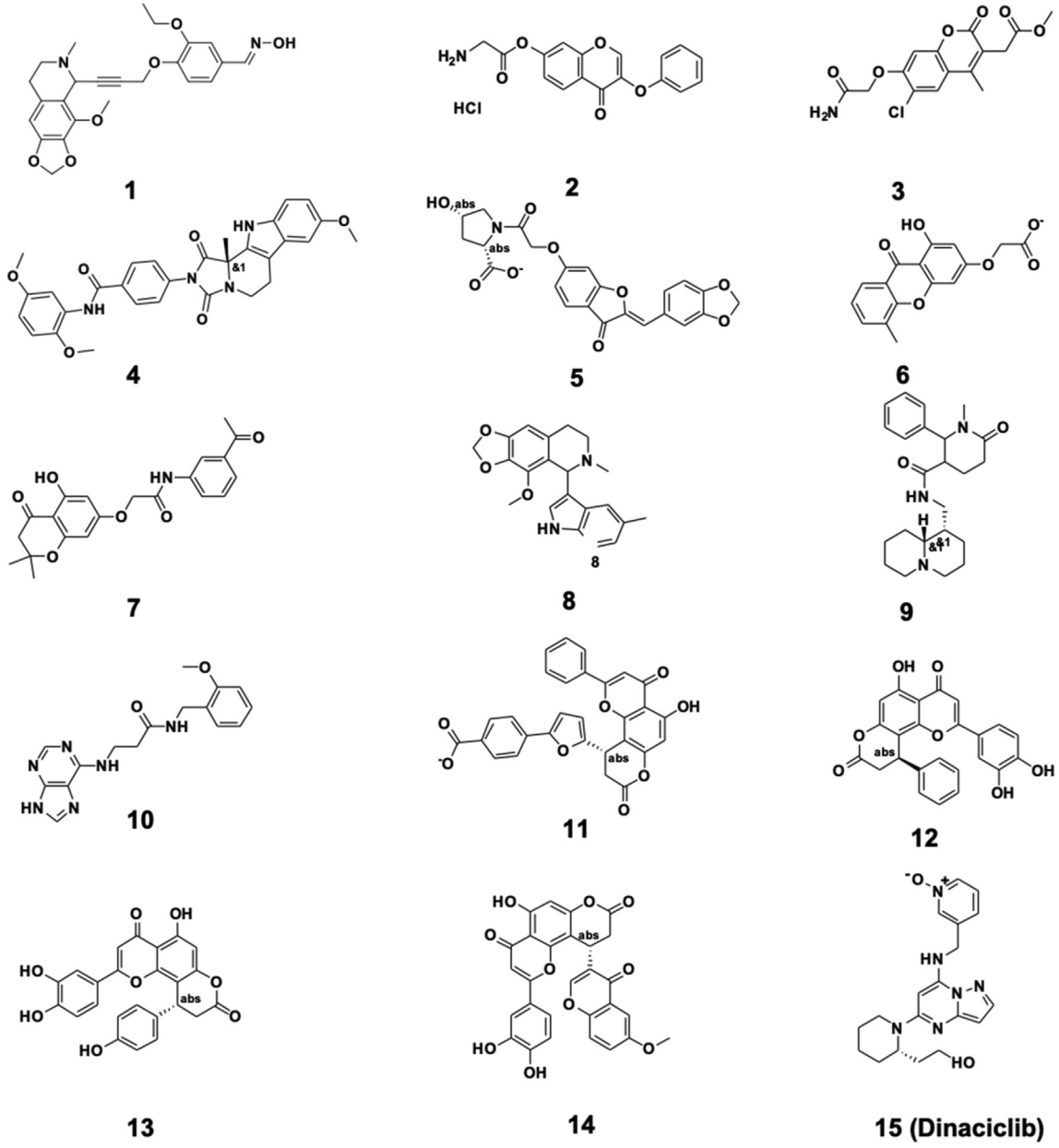


**Figure 1** Chemical structures of compounds **1**—**14** identified by virtual screening, and positive control compound (**15**).

## Compound 1 selectively binds with CDK9 and inhibits the CDK9-cyclin T1 PPI

To explore whether compound **1** engages with CDK9 or cyclin T1, the cellular thermal shift assay (CETSA) was conducted (Fig. 4A). MDA-MB-231 cell lysates were incubated with compound **1** (10 μM) for 30 min, CDK9, cyclin T1, and β-actin levels in the soluble fraction were detected by Western blotting (Fig. 4B, D). CDK9 in cell lysates treated with compound **1** were significantly stabilized ($\Delta T_m$: 5.2°C). This result indicated that compound **1** can engage CDK9 even in the cellular lysate environment. Due to the high sequence identity among the CDK family, selectivity is an important issue for screening CDK inhibitors. CDK9 shares a high degree of homology with CDK1, CDK2, CDK5, and CDK12.[30] Therefore, we also detected the binding affinity of compound **1** against CDK1, CDK2, CDK5, and CDK12 in MDA-MB-231 lysates using CETSA (Fig. 4E). The results showed that compound **1** exhibited negligible thermal stabilization of the other CDK members, indicating that compound **1** had high selectivity for CDK9 (Fig. 4F, J).

Given the promising activity of compound **1** at inhibiting CDK9-cyclin T1 activity, its *in cellulo* mechanism of action was next explored. A co-IP experiment was conducted to evaluate the effect of compound **1** on the interaction between CDK9 and cyclin T1 in MDA-MB-231 cells (Fig. 4K). The result showed that compound **1** could disrupt the interaction between CDK9 and cyclin T1 *in cellulo*, as indicated by the reduction of cyclin T1 co-precipitated with CDK9. Mechanistically, compound **1** and **15** may act as different inhibition mechanisms in the cellular context. Our

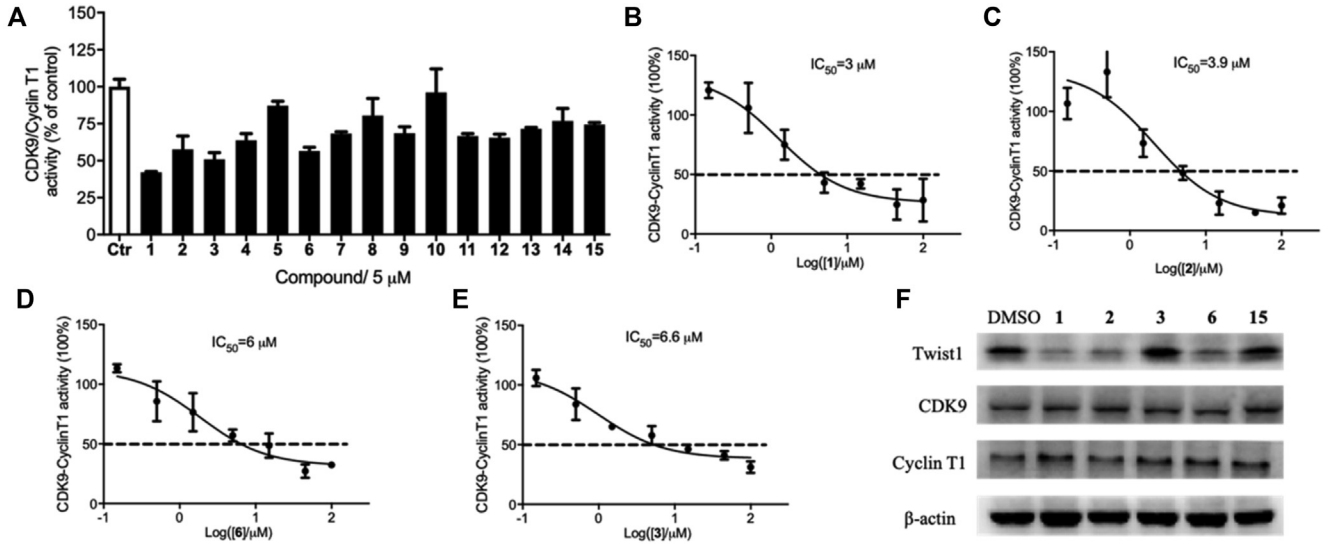


**Figure 2** Compound **1** was identified as the top CDK9-cyclin T1 inhibitor. **(A)** The effect of compounds **1**—**14** on the CDK9-cyclin T1 activity was determined by a chemiluminescence assay. **(B—E)** Compounds **1**, **2**, **3**, and **6** inhibited CDK9-cyclin T1 activity in a dose-dependent manner as measured using a chemiluminescence assay. **(F)** The effect of candidate compounds **1**, **2**, **3**, **6**, and **15** on Twist1 expression as detected by Western blotting.

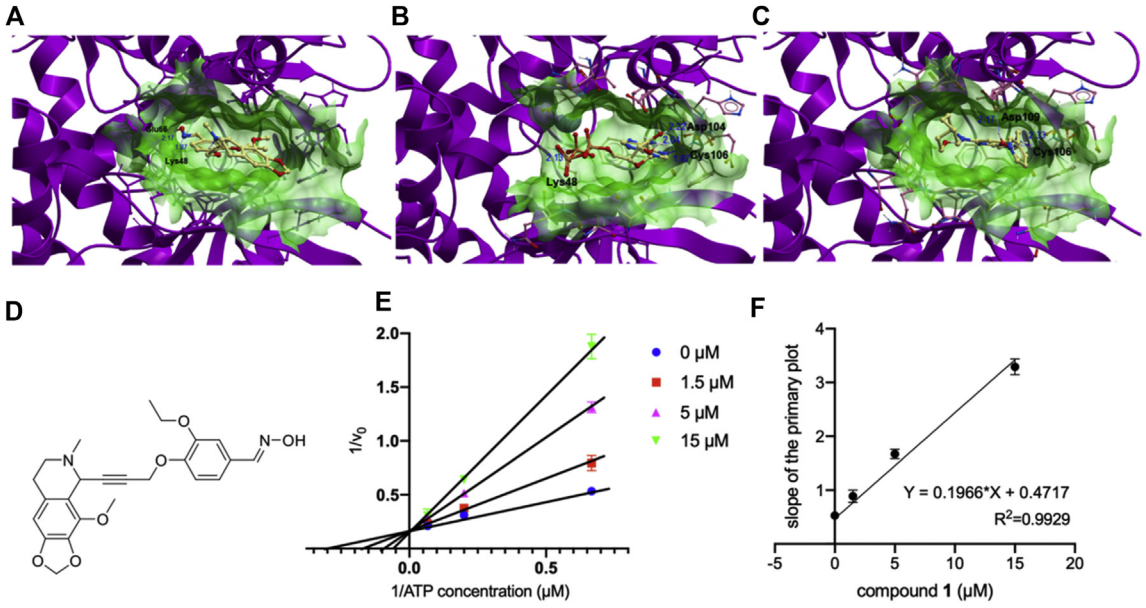


**Figure 3** Low-energy binding conformation of (A) compound **1** (PDB: 6GZH) (B) ATP (PDB: 3BLQ) and (C) dinaciclib (15) (PDB: 6GZH) generated by *in silico* docking. **(A—C)** CDK9 is displayed in ribbon form. Compound **1** (A), ATP (B), and dinaciclib (C) are depicted as a ball-and-stick models showing carbon (yellow), hydrogen (grey), oxygen (red), and nitrogen (blue) atoms. H-bonds are indicated as blue lines. The binding pocket of the CDK9 is represented as a translucent surface. **(D)** Chemical structure of compound **1**. **(E)** Lineweaver—Burk plot of enzyme activity measured at different ATP concentrations in the presence of different concentrations of compound **1**. **(F)** Secondary Lineweaver—Burk plot to obtain the $K_i$ value.

CETSA and co-IP results indicate that compound **1** binds with CDK9 and blocks the CDK9-cyclin T1 PPI, with superior potency compared to compound **15**. On the other hand, compound **15** has been reported as a pan-CDK inhibitor, and may have CDK9 inhibitory activity without significantly disrupting the CDK9-cyclin T1 PPI.[31] This is supported by our molecular modeling results, which show a different binding of compound **1** to **15** in the CDK9-cyclin T1 complex.

## Compound 1 inhibits the transcription of EMT and CSCs biomarkers

Previous research has demonstrated that the CDK9-cyclin T1 network plays a critical role in regulating EMT and CSCs by regulating the expression of EMT/CSC-related genes (such as *Twist1*, *Snail*, and *OCT4*) via directly binding to their *cis*-acting element.[20,32] The effect of

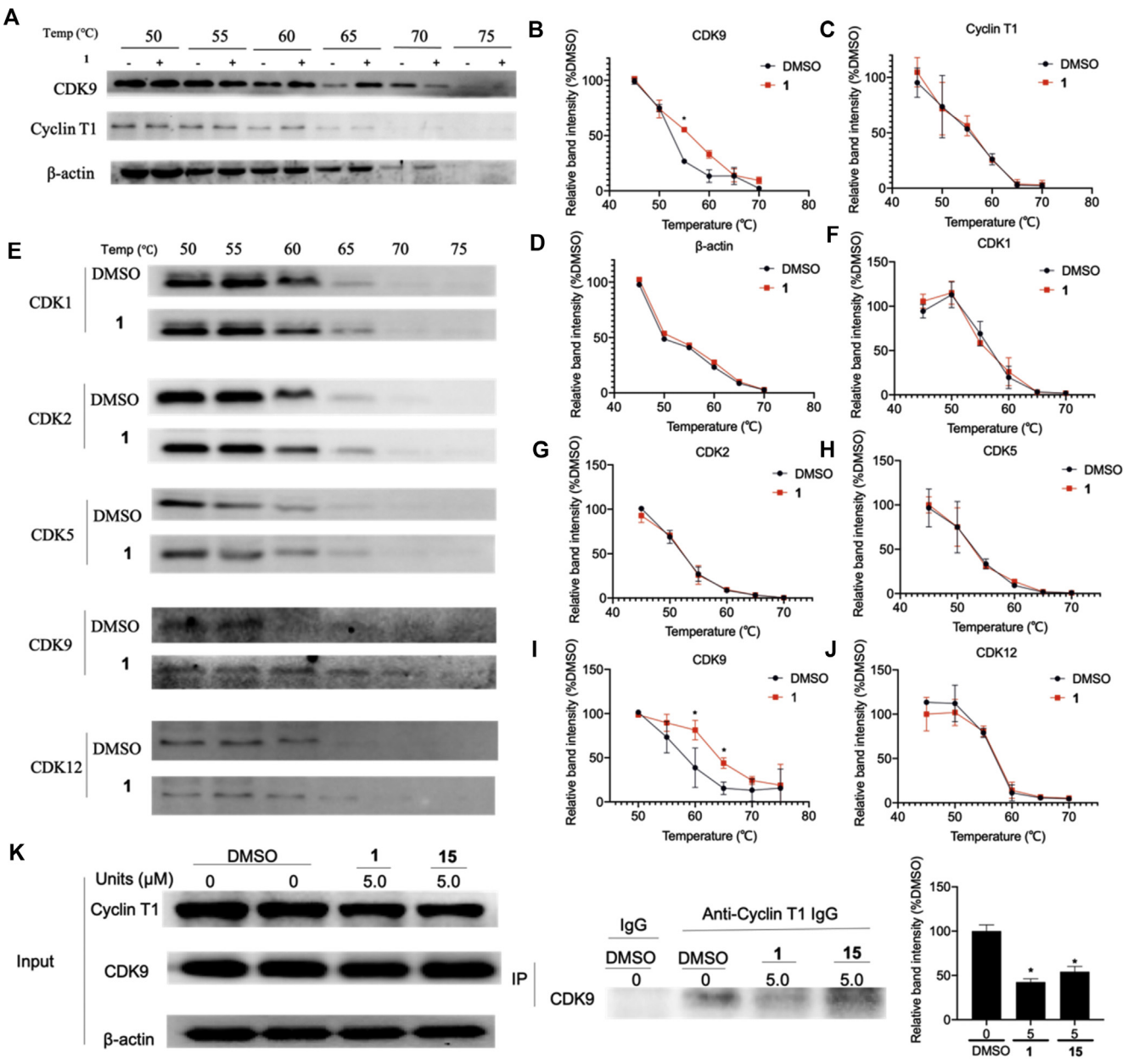


**Figure 4** Compound **1** can selectively bind with CDK9 and by block the CDK9-cyclin T1 interaction in *in cellulo*. **(A)** MDA-MB-231 cell lysates were treated with compound **1** at 10.0 μM CDK9, Cyclin T1, and β-actin content in the soluble fraction were detected by Western blotting. **(B—D)** Densitometry analysis of CDK9, cyclin T1, and β-actin content. **(E)** MDA-MB-231 cell lysates were treated with compound **1** at 10.0 μM CDK1, CDK2, CDK5, CDK9, and CDK12 content in the soluble fraction were detected by Western blotting. **(F—J)** Densitometry analysis of CDK content. **(K)** Effect of compound **1** on CDK9-Cyclin T1 interaction as revealed by co-IP assay. Data are represented as mean ± SD. $^*P < 0.05$ *vs.* DMSO group, (Student's *t* test).

compound **1** on the binding of CDK9-cyclin T1 to the *cis*-acting elements of these genes (primers in Table S1) was explored using the chromatin immunoprecipitation (ChIP) assay (Fig. 5A—C). After 12 h treatment with compound **1** (5 μM), MDA-MB-231 cells were harvested, cross-linked, and immunoprecipitated with the anti-CDK9 antibody. The results showed that compound **1** reduced the occupation of CDK9-cyclin T1 PPI at the upstream regulatory elements of EMT (*Twist1* and *Snail)* and CSCs (*OCT4)* genes in TNBC cells.

Given the ability of compound **1** to decrease occupany of CDK9-cyclin T1 PPI at the upstream regulatory elements of EMT and CSC-related genes, we next explored its effect on the transcription and translation of those genes. Specifically, compound **1** significantly decreased *Twist1*, *Snail*, and *OCT4* in MDA-MB-231 (Fig. 5D, F) and MDA-MB-468 (Fig. 5G—I) cells at the transcription level as revealed using qPCR. Moreover, compound **1** decreased the protein expression of EMT (Snail and Twist1) and CSC (OCT4, CD44, and CD133) biomarkers in MDA-MB-231 and MDA-MB-

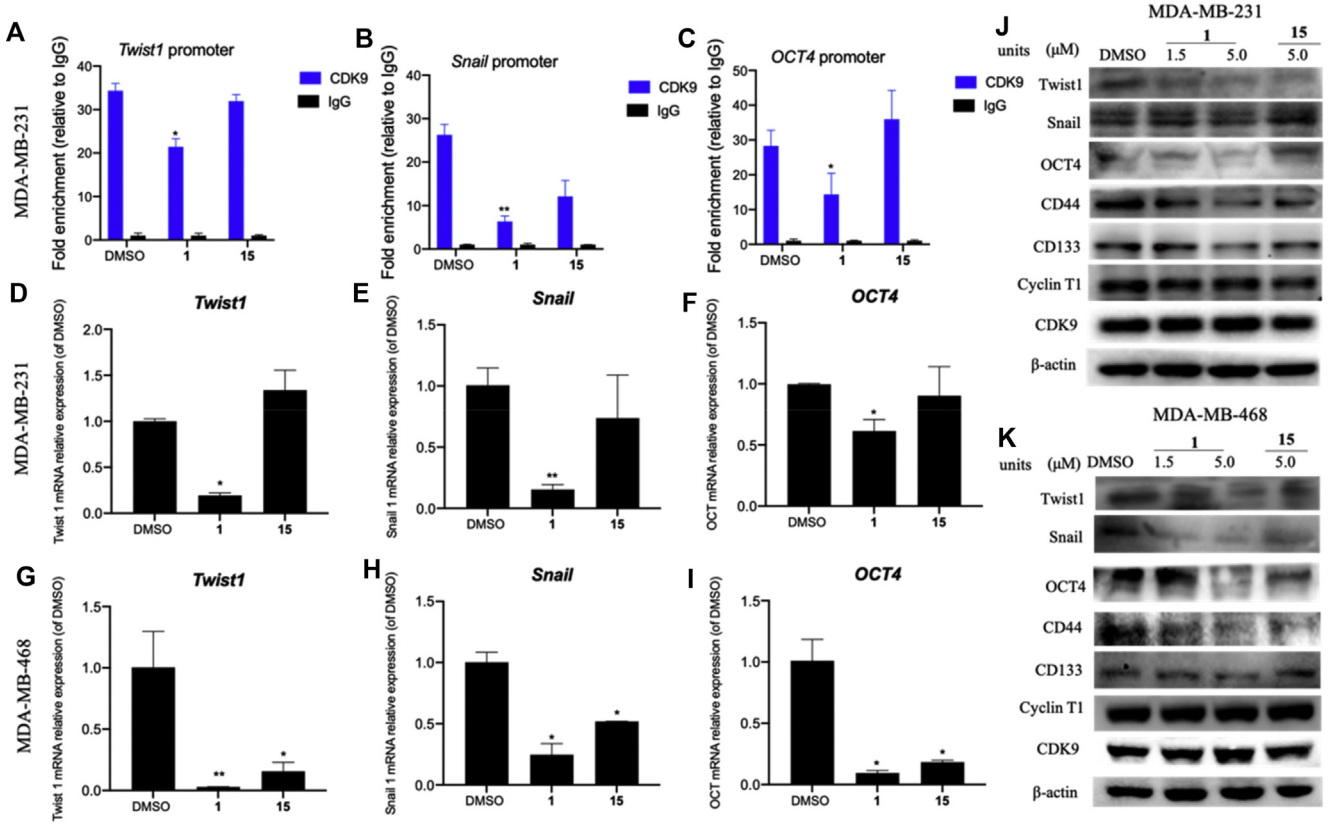


**Figure 5** Compound **1** inhibited *Snail*, *Twist1*, and *OCT4* at both transcriptional and translational levels. **(A—C)** Compound **1** inhibited CDK9 at promoters of *Snail*, *Twist1*, and *OCT4* gene in MDA-MB-231 cells. ChIP assay was conducted with the primary antibody against CDK9 and IgG. **(D—F)** Transcriptional levels of *snail*, *Twist1*, and *OCT4* in MDA-MB-231 and MDA-MB-468 cells treated with compound **1** or **15** were measured by qPCR. **(G—K)** Compound **1** inhibited the MDA-MB-231 and MDA-MB-468 stemness by targeting CDK9. Data are represented as mean ± SD. $^{*}P < 0.05$, $^{**}P < 0.01$ *vs.* DMSO group, (Student's *t* test).

468 cells in a dose-dependent manner as measured by Western blotting (Fig. 5J, K). Although CD44 and CD133 are not directly regulated by the CDK9-cyclin T1 complex, they are common biomarkers of CSCs in TNBC.[5] Taken together, these results indicate that compound **1** impairs the expression of EMT and CSC-related genes at both transcriptional and translational levels in TNBC cells.

To study whether compound **1** regulates gene expression at the transcriptional or translational level, the expression assays were repeated in the presence of either a transcription inhibitor (ActD) or a translation inhibitor (CHX). Cells were pretreated with or without the presence of transcription inhibitor ActD to block the transcription progress. The results showed that ActD pre-treatment abolished the inhibitory effect of compound **1** on Twist1, Snail, and OCT4 expression, suggesting that compound **1** downregulated their expression at the transcriptional level (Fig. 6B, D). In addition, cells pretreated with compound **1** were incubated with the translation inhibitor CHX to study the effect of compound **1** on the protein stability of Twist1, Snail, and OCT4 (Fig. 6E). The results showed that compound **1** exhibited no significant effect on OCT4, Twist1, and Snail stability compared to the DMSO group in CHX treated cells (Fig. 6F—H), suggesting that compound **1** did not interfere with the post-translational process. Taken together, these results indicate that compound **1** acts via regulating transcription of OCT4, Twist1, and Snail expression rather than translation.

Mammary epithelial cells of MCF-10A exhibit similar characteristics of TNBC cancer cell lines and are usually used to investigate EMT pathways in breast cancer.[33,34] Therefore, we evaluated the EMT signature in MCF-10A cells, which include EMT-related proteins underlying the CDK9-cyclin T1 pathway and migration ability (Fig. S2). The results showed that compound **1** could suppress Twist1 and Snail protein levels in a dose-dependent manner (Fig. S2a—c). In addition, compound **1** decreased the migration activity of MCF-10A cells (Fig. S2d—e). All of these results indicated that compound **1** may reverse EMT and reduce cancer cell stemness via blocking the CDK9-cyclin T1 PPI and thus downregulating the levels of associated genes.

## CDK9-dependent inhibition of EMT and CSCs biomarkers by compound 1

To further verify whether compound **1** targets CDK9 to exert its effects, a knockdown experiment was performed (Fig. 7A). The results showed that compound **1** or CDK9 siRNA treatment significantly reduced EMT biomarkers

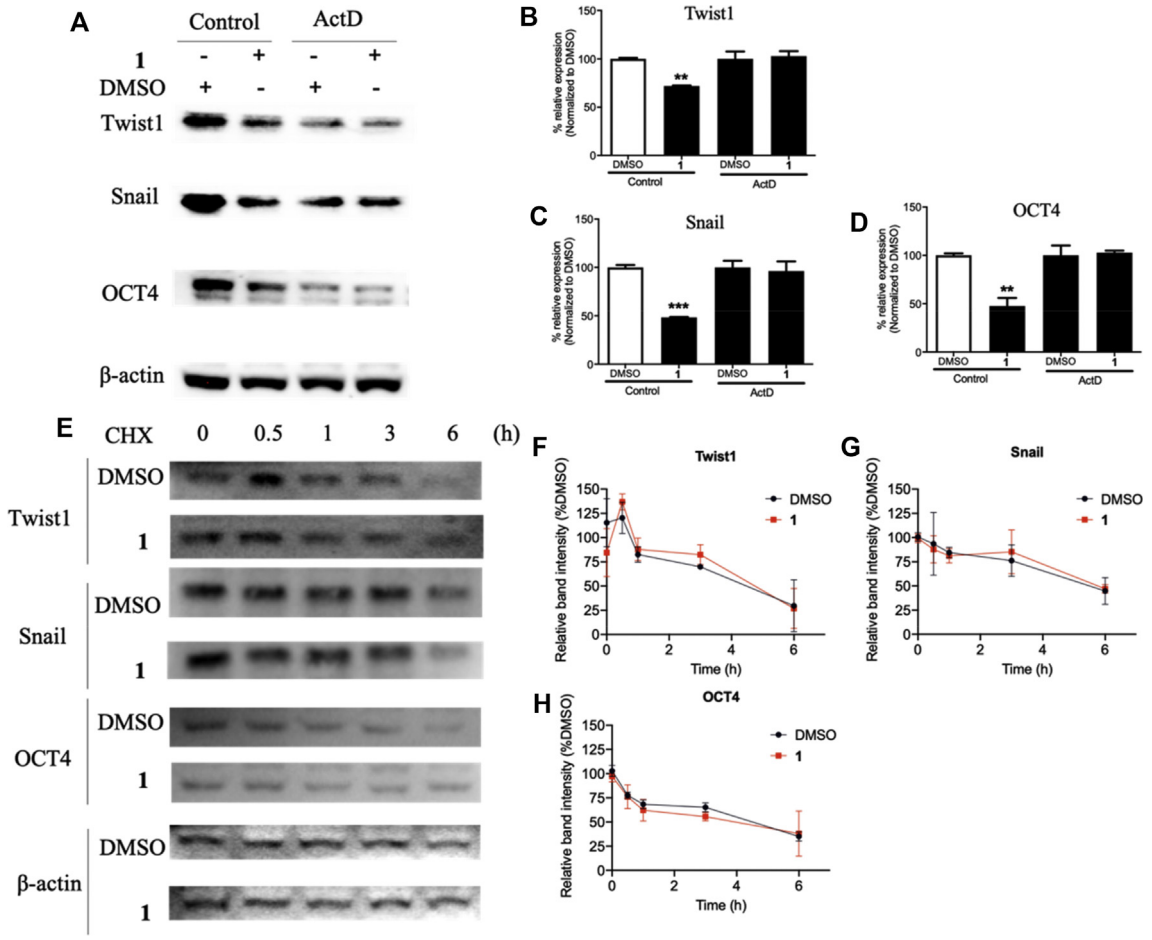


**Figure 6** Compound **1** decreased OCT4, Twist1, and Snail expression by a transcriptional mechanism. **(A)** MDA-MB-231 cells were pretreated with 0.1 μM ActD for 1 h and then treated with 5 μM of compound **1** for 12 h. Twist1, Snail, OCT4, and β-actin were analyzed by Western blotting. **(B—D)** Quantification analysis of Twist1, Snail, and OCT4 in Western blotting. Data are represented as mean ± SD. $^{**}P < 0.01$, $^{***}P < 0.005$ *vs* DMSO group, (Student's *t* test). **(E)** Protein stability of Twist1, Snail, and OCT4 in MDA-MB-231 cells. Cells were treated with 5 μM of compound **1** for 12 h and then treated with CHX (5 μM) for 0, 0.5, 1, 3, 6 h. Equal amounts of whole cell lysates were analyzed by Western blotting with Twist1, Snail, OCT4, and β-actin. **(F—H)** Densitometry analysis of Twist1, Snail, and OCT4 content.

(Snail and Twist1) and CSC biomarkers (CD44 and CD133) in MDA-MB-231 TNBC cells (Fig. 7B, F). Importantly, compound **1** induced no significant decrease in CSC and EMT protein levels compared to the DMSO group in CDK9 knockdown cells. These results indicated that the suppression of EMT and CSC biomarkers by compound **1** *in cellulo* could be associated, at least in part, with the targeting of CDK9.

To further study whether compound **1** acts through targeting CDK9, the CDK9 plasmid was transfected into MDA-MB-231 cells. EMT biomarkers (Snail and Twist1) were detected and the cytotoxicity of compound **1** was evaluated in both knockdown and CDK9-overexpressing cells using the MTT assay (Fig. S3). The results indicated that CDK9-overexpressing cells were more sensitive to EMT biomarker (Snail and Twist1) reduction and cytotoxicity induced by compound **1** compared to parental cells and knockdown cells, suggesting that compound **1** targets CDK9 to exert its biological effects.

## Compound 1 effectively suppresses 3D spheroids formation by inhibiting the CDK9-cyclin T1 pathway

3D tumor spheres possess characteristic features of CSCs, such as a high capacity of self-renewal, metastasis, and differentiation.[35] 3D tumor spheres also express higher levels of CSC and EMT genes than 2D monolayer cells.[36] Therefore, we used a 3D cell culture assay to evaluate the effect of compound **1** on spheroid formation and the self-renewal potential of tumor sphere cells. MDA-MB-231 and MDA-MB-468 cells were seeded in low-cell attachment dishes to stimulate spheroid formation, then incubated with 10 or 30 μM of compound **1** or DMSO for two weeks (Fig. 8A, B). The results indicated that 10 and 30 μM of compound **1** can inhibit 3D tumor growth in TNBC cells (Fig. 8C, D).

TNBC with a high percentage of the CSC biomarkers $CD44^{+}/CD24^{-}$ have a more aggressive phenotype with a

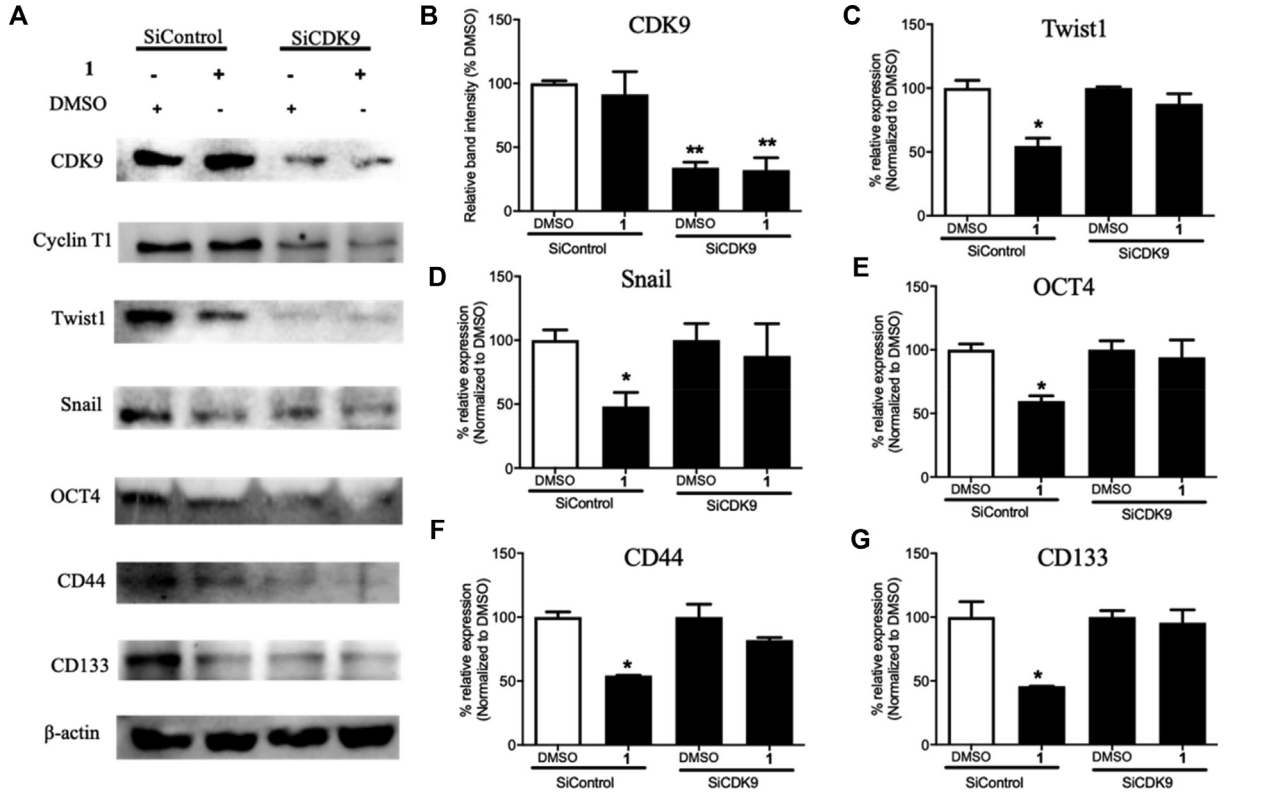


**Figure 7** Compound **1** directly abrogated CDK9 activity via disrupting the CDK9-cyclin T1 PPI and negatively regulating its downstream genes. **(A)** CDK9 siRNA treatment produced efficient target knockdown in MDA-MB-231 cells. CDK9, cyclin T1, Twist1, Snail, OCT4, CD44, CD133, and $\beta$-actin were blotted to control for total protein levels. SiControl: SiRNA control; SiCDK9: SiRNA CDK9. **(B—F)** Quantification analysis of CDK9, Twist1, Snail, OCT4, CD44, and CD133 in Western blot. Data are represented as mean $\pm$ SD. $^{*}P < 0.05$, $^{**}P < 0.01$ *vs.* DMSO group, (Student's *t* test).

higher capacity for cell proliferation and metastasis.[37] Hence, the $CD44^{+}/CD24^{-}$ populations were detected after treating MDA-MB-231 cells with compound **1** or **15** (5 μM). The results showed that compound **1** can decrease $CD44^{+}/CD24^{-}$ stem-like populations in MDA-MB-231 cells (Fig. 8E). Taken together, our findings suggest that compound **1** can suppress cell stemness and cell renewal, presumably through inhibiting CDK9-cyclin T1 signaling thus down-regulating the transcription and expression of EMT (Snail and Twist1) and CSC (OCT4, CD44, and CD133) genes (Fig. 5A—K).

## Compound 1 exhibits the anti-proliferation activity and anti-migration activity in TNBC cells

EMT and CSCs control various cellular processes such as migration, invasion, and apoptosis.[36] Moreover, the CDK9-cyclin T1 complex is critical for cell proliferation and knockdown of CDK9 suppresses cell proliferation and migration.[38,39] Hence, the cytotoxicity, proliferation, and migration effect of compound **1** on both breast cancer cells and normal breat epithelial cells were evaluated.

The cytotoxicity of compound **1** was investigated in different breast cancer cell lines, as well as human normal cell lines by the MTT assay. Compound **1** exhibited potent cytotoxicity against the TNBC (MDA-MB-231, MDA-MB-468 and BT549) cell lines with estimated $IC_{50}$ values of 6.2, 7.4, and 12.6 μM, while showing lower toxicity against non-TNBC breast cancer cell lines (T47D: 52.5 μM; MCF-10A: 35.5 μM). Moreover, compound **1** showed no obvious activity ($IC_{50} \geq 100$ μM) against the human normal cell lines LO2 and HEK 293T (Fig. 9A). Similarly, the colony formation assay demonstrated that compound **1** could inhibit the proliferation of MDA-MB-231 and MDA-MB-468 cells (Fig. 9B—E). As a comparison, we also determined the cytotoxicity of the positive control dinaciclib (**15**) in MDA-MB-231 (0.007 μM), MDA-MB-468 (0.01 μM), BT549 (0.026 μM) cells, MCF-10A (0.03 μM), T47D (0.33 μM), LO2 (0.02 μM), and HEK 293T (0.04 μM) cells using the MTT assay (Fig. S4). The therapeutic index of compound **1**, which was defined as the ratio of $IC_{50}$ values of normal cells against MDA-MB-231 cells, was at least 16 for both normal cell lines, whereas compound **15** exhibited lower therapeutic indices of 2.9 and 5.7 for LO2 and HEK 293T respectively over MDA-MB-231. This showed that while compound **1** had lower cytoxicity than dinaciclib (**15**) against breast cancer cells, it possessed superior selectivity for TNBC cells over normal cells.

Reports have suggested that CDK1, 2, and 6 together with their cyclin subunits are responsible for cell cycle progress, while CDK7 and 9 are responsible for transcription.[40] In addition, it has been reported that CDK9-cyclin T1 activity are not cell cycle regulated.[15,41] Consistent with this, our

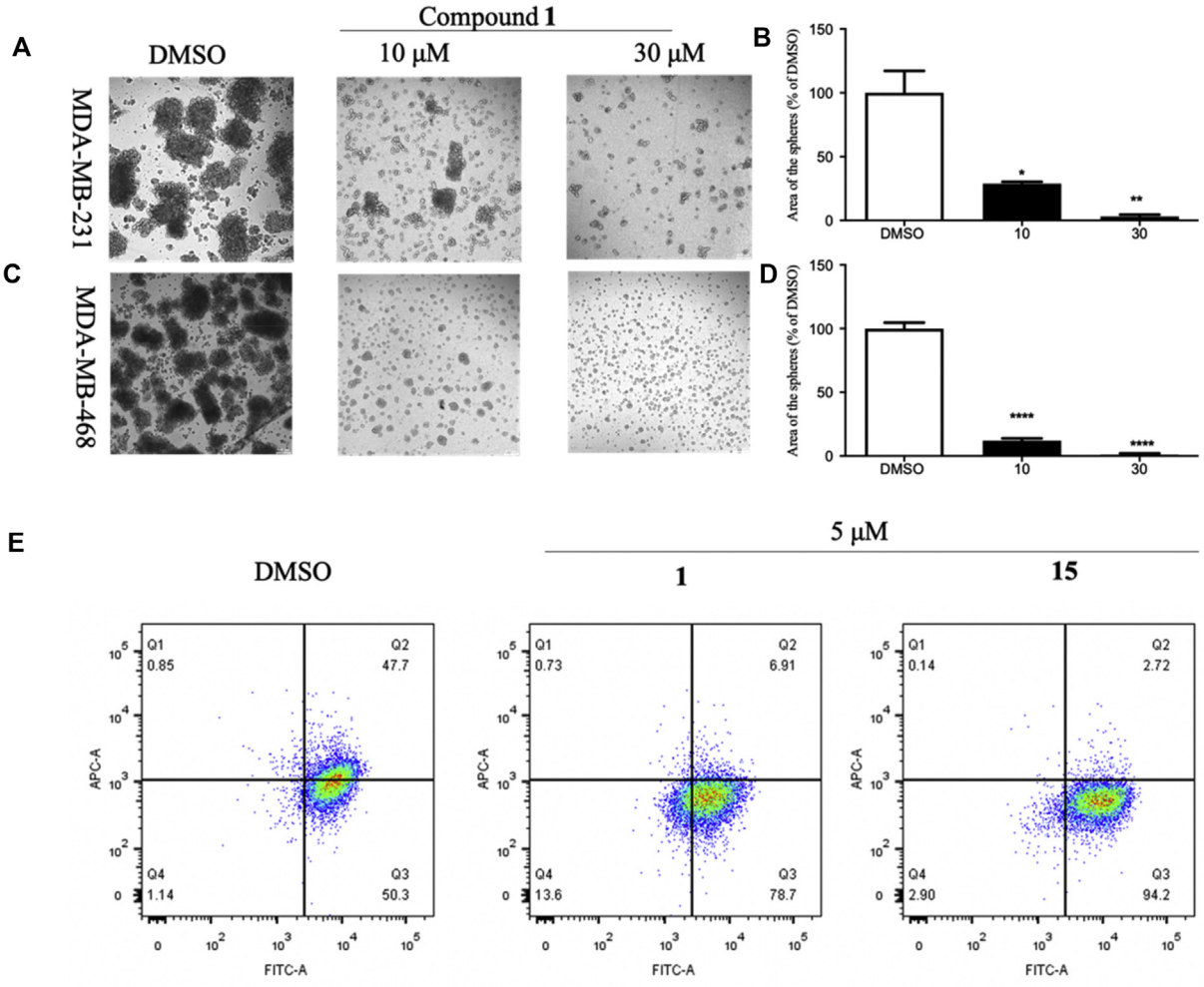


**Figure 8** Compound **1** inhibited TNBC stemness by targeting CDK9. **(A, C)** Compound **1** reduced 3D tumor sphere formation in MDA-MB-231 and MDA-MB-468 cells. Scale bars represent 100 μm. **(B, D)** Relative tumor sphere volume. **(E)** Effect of compound **1** or **15** (5 μM, 12 h) on $CD44^{+}/CD24^{-}$ populations by flow cytometric analysis. Data are represented as mean ± SD. $^{*}P < 0.05$, $^{**}P < 0.01$, $^{****}P < 0.0001$ *vs.* DMSO group, (Student's *t* test).

results showed that compound **1** had no significant effect on cell cycle progress, suggesting that the inhibition of the CDK9-cyclin T1 PPI and downstream EMT and CSCs markers by compound **1** is not dependent on the cell cycle (Fig. S5).

Finally, the effect of compound **1** on the migration ability of MDA-MB-231 and MDA-MB-468 was also studied. The results showed that compound **1** showed dose-dependently inhibited migration activity in TNBC cells (Fig. 9F—I). Taken together, these results indicated that by antagonizing the CDK9-cyclin T1 interaction *in cellulo*, compound **1** can exert anti-proliferation and anti-migration phenotypes.

## Discussion

Kinases are very important targets for drug discovery due to their pivotal roles in human diseases, including cancer.[42] CDK9 has important roles in regulating basal gene transcriptional homeostasis, as well as EMT and CSC phenotypes.[18,43] Since CDK9 is often dysregulated in cancer, it is emerging as an important target in cancer therapy.[16] Targeting a PPI to directly or indirectly to regulate protein kinase activity could be an alternative strategy to inhibit the CDK9-cyclin T1 activity.[44] Since cyclin T1 is regulatory subunit that activates the activity of CDK9, developing selective PPI inhibitors for the CDK9-cyclin T1 PPI could be a viable approach for treating cancer. A previous study performed computational analysis of the CDK9-cyclin T1 complex to design peptide and small molecule inhibitors binding to the CDK9-cyclin T1 interface or the ATP-binding pocket.[45,46] Another report described the *in silico* docking of drugs to the ATP site of CDK9-cyclin T1.[47] However, to our knowledge, no CDK9-cyclin T1 PPI inhibitor has yet been reported for targeting TNBC metastasis.

Natural products provide diverse bioactive structural motifs for drug screening.[48] Some natural products have also shown inhibitory activity against CDK9 kinase.[18] For instance, flavopiridol is a semisynthetic flavonoid with inhibitory activity against CDK9.[15] Seliciclib, a CDK2/7/9 inhibitor in clinical trials, comes from the cotyledons of radish.[12] Wogonin is a natural flavone that targets CDK9 by

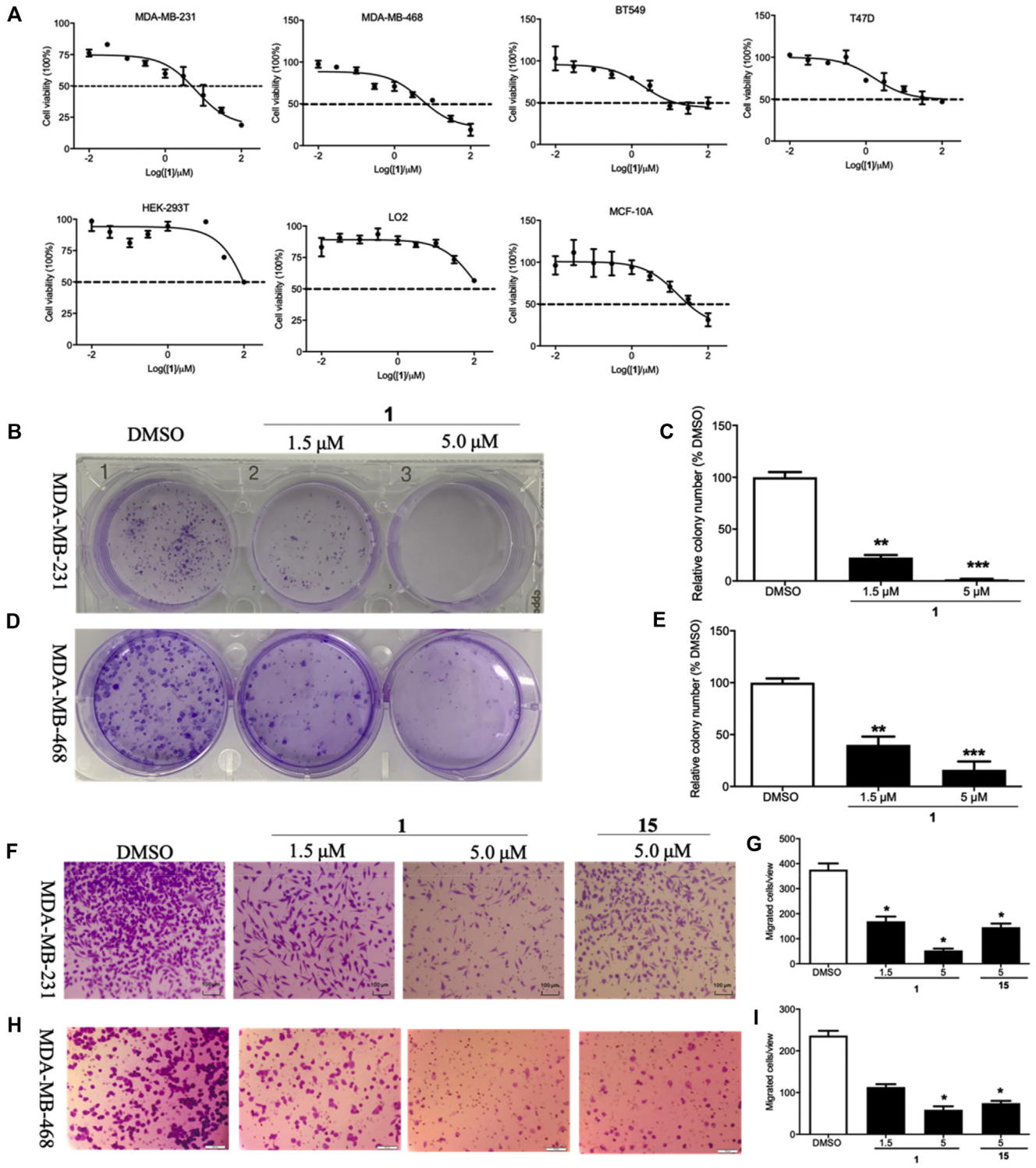


**Figure 9** Compound **1** induced cell toxicity and inhibited cell migration in MDA-MB-231 and MDA-MB-468 cells. **(A)** The cytotoxicity effect of compound **1** on MDA-MB-231, MDA-MB-468, BT549, T47D, HEK 293T, LO2, and MCF-10A cells. Cells were treated with indicated concentrations of **1** for 72 h and cytotoxicity results were determined by MTT assay. **(B, D)** 5 μM of compound **1** inhibited MDA-MB-231 and MDA-MB-468 cell proliferation as detected by a colony formation assay. **(C, E)** Relative analysis of colony number compared to DMSO. **(F, H)** Cell migration effect of compound **1** on MDA-MB-231 and MDA-MB-468 cells treat with 1.5 μM, 5 μM, or **15**. **(G, I)** Quantitative analysis of migration cells. Data are represented as mean ± SD. $^{*}P < 0.05$, $^{**}P < 0.01$, $^{***}P < 0.001$ *vs.* DMSO group, (Student's *t* test).

engaging the ATP-binding pocket.[49] At the same time, virtual screening has arisen as a viable and cost-efficient approach to supplement traditional drug discovery efforts and is particularly relevant for natural products where supplies may be scarce.

In this paper, we have identified the tetrahydroisoquinoline compound **1** as a potent CDK9-cyclin T1 PPI inhibitor from a 280,000-compound chemical library of natural product/natural product-like compounds using *in silico* screening against the CDK9 active site. Although tetrahydroisoquinoline-based compounds have been reported as anticancer agents,[50] no pharmacological research has been documented to shed light on their potential mechanism. The ability of compound **1** to engage CDK9 in cell lysates was confirmed using CETSA. Moreover, compound **1** showed stronger engagement to CDK9 compared to CDK1, CDK2, CDK5, and CDK12 in the CETSA assay, indicating high selectivity for CDK9. CDK family members have high sequence similarities and most CDK inhibitors usually lack selectivity, which leads to toxicity and off-target effects.[42] In particular, CDK1, CDK2, CDK5, CDK12 shares a high degree of homology with CDK9.[30]

An *in vitro* chemiluminescence assay demonstrated that compound **1** acted as a CDK9-cyclin T1 kinase inhibitor. Molecular modeling analysis suggested that compound **1** can target the ATP-binding pocket of CDK9, which was supported by kinetics analysis showing an ATP-competitive mode of inhibition. Interestingly, *in cellulo* co-immunoprecipitation experiments showed that compound **1** also disrupted the CDK9-cyclin T1 PPI. Substantial evidence has shown that the active site of protein kinases is allosterically regulated, while conversely, targeting the ATP site can also alter the conformation of the regulatory regions allosterically, resulting in the modulation of PPIs.[51] Some ATP-competitive inhibitors have been reported to modulate the PPIs of kinases.[52,53] We speculate that the distinct binding mode of compound **1** relative to ATP or dinaciclib (**15**) as shown in the molecular modeling results may account for its unique ability to disrupt the CDK9-cyclin T1 PP1.

Wang et al[18] reported a series of CDK9 inhibitors with inhibitory activity against CSCs for cancer treatment. Moreover, the CDK9-cyclin T1 complex controls the expression of EMT regulators to promote TNBC progression.[54] To explore the mechanism of activity of Compound **1** against TNBC, we detected EMT and CSC biomarkers by ChIP, qPCR, Western blotting, and flow cytometric analysis. Pleasingly, compound **1** showed promising activity against decreasing EMT and CSC biomarkers with comparable activity compared to the clinical CDK inhibitor dinaciclib (**15**). Compound **1** weakened the amplification of the *Twist1*, *Snail* and *OCT4* promoters by CDK9, leading to the abrogation of Twist1, Snail and OCT4 at the transcriptional levels. To further investigate the inhibitory effects of compound **1** on Twist1, Snail and OCT4, we knocked down CDK9 which directly regulates these genes. The results indicated that compound **1** suppressed the levels of EMT and CSC biomarkers mainly by targeting CDK9. Compound **1** also reduced the volume of cultured 3D tumor spheres, a model for the CSC and EMT phenotype.[35] Breast cancer cells with characteristics of CSCs and EMT have significantly enhanced migration ability.[55] Compound **1** exhibited dose-dependent anti-migration ability, suggesting that CDK9 may act as the important regulator of EMT and CSC characteristics. Finally, a cytotoxicity assay showed that compound **1** potently inhibited TNBC cells, with lower toxicity against normal human cells compared to dinaciclib **15**.

## Conclusions

In conclusion, we have discovered the first tetrahydroisoquinoline-based CDK9-cyclin T1 inhibitor based on virtual screening. In addition to inhibiting CDK9 kinase activity, compound **1** also disrupted the CDK9-cyclin T1 PPI. By the use of compound **1**, our results have revealed a new mechanism of EMT and CSC induction via the CDK9-cyclin T1 pathway in TNBC cells. Taken together, our results demonstrate the importance of CDK9 as a pharmacological target in TNBC and showcase the potential of compound **1** as a new lead for developing more selective and potent CDK9-cyclin T1 PPI inhibitors.

## Author contributions

Shasha Cheng and Guan-Jun Yang: Data acquisition and analysis, manuscript preparation. Wanhe Wang: Data acquisition and analysis. Dik-Lung Ma and Chung-Hang Leung: Concept and design, data analysis, manuscript editing.
We ensure that all appropriate contributors are listed as authors and that all authors have agreed to the manuscript's content and its submission to *Genes & Diseases*.

## Conflict of interests

The authors declare no conflict of interest.

## Funding

This work was supported by the Health and Medical Research Fund (No. HMRF/14150561); the National Natural Science Foundation of China (No. 201575121 and 21775131); the Hong Kong Baptist University Century Club Sponsorship Scheme 2020, Teaching Development Fund (No. TDG/1920/02); the Science and Technology Development Fund, Macau SAR, China (File no. 0072/2018/A2 and 0007/2020/A1); SKL-QRCM(UM)-2020-2022; the University of Macau, China (MYRG2019—00002—ICMS).

## Appendix A. Supplementary data

Supplementary data to this article can be found online at https://doi.org/10.1016/j.gendis.2021.06.005.

## References

1. Wahba HA, El-Hadaad HA. Current approaches in treatment of triple-negative breast cancer. *Cancer Biol Med*. 2015;12(2):106—116.
2. Yang GJ, Zhong HJ, Ko CN, et al. Identification of a rhodium (iii) complex as a Wee1 inhibitor against TP53-mutated triple-

negative breast cancer cells. *Chem Commun*. 2018;54(20): 2463—2466.
3. Doherty MR, Cheon H, Junk DJ, et al. Interferon-beta represses cancer stem cell properties in triple-negative breast cancer. *Proc Natl Acad Sci U S A*. 2017;114(52):13792—13797.
4. Park SY, Choi JH, Nam JS. Targeting cancer stem cells in triple-negative breast cancer. *Cancers (Basel)*. 2019;11(7):965.
5. Singh SR. Gastric cancer stem cells: a novel therapeutic target. *Cancer Lett*. 2013;338(1):110—119.
6. Lin L, Jou D, Wang Y, et al. STAT3 as a potential therapeutic target in ALDH+ and CD44+/CD24+ stem cell-like pancreatic cancer cells. *Int J Oncol*. 2016;49(6):2265—2274.
7. Agliano A, Calvo A, Box C. The challenge of targeting cancer stem cells to halt metastasis. *Semin Cancer Biol*. 2017;44:25—42.
8. Raz R, Lee CK, Cannizzaro LA, d'Eustachio P, Levy DE. Essential role of STAT3 for embryonic stem cell pluripotency. *Proc Natl Acad Sci U S A*. 1999;96(6):2846—2851.
9. Kalluri R, Weinberg RA. The basics of epithelial-mesenchymal transition. *J Clin Invest*. 2009;119(6):1420—1428.
10. Bleau AM, Agliano A, Larzabal L, de Aberasturi AL, Calvo A. Metastatic dormancy: a complex network between cancer stem cells and their microenvironment. *Histol Histopathol*. 2014;29(12):1499—1510.
11. Mani SA, Guo W, Liao MJ, et al. The epithelial-mesenchymal transition generates cells with properties of stem cells. *Cell*. 2008;133(4):704—715.
12. Cassandri M, Fioravanti R, Pomella S, et al. CDK9 as a valuable target in cancer: from natural compounds inhibitors to current treatment in pediatric soft tissue sarcomas. *Front Pharmacol*. 2020;11:1230.
13. Brisard D, Eckerdt F, Marsh LA, et al. Antineoplastic effects of selective CDK9 inhibition with atuveciclib on cancer stem-like cells in triple-negative breast cancer. *Oncotarget*. 2018; 9(99):37305—37318.
14. Bacon CW, D'Orso I. CDK9: a signaling hub for transcriptional control. *Transcription*. 2019;10(2):57—75.
15. Baumli S, Lolli G, Lowe ED, et al. The structure of P-TEFb (CDK9/cyclin T1), its complex with flavopiridol and regulation by phosphorylation. *EMBO J*. 2008;27(13):1907—1918.
16. Schlafstein AJ, Withers AE, Rudra S, et al. CDK9 expression shows role as a potential prognostic biomarker in breast cancer patients who fail to achieve pathologic complete response after neoadjuvant chemotherapy. *Int J Breast Cancer*. 2018; 2018:6945129.
17. McLaughlin RP, He J, van der Noord VE, et al. A kinase inhibitor screen identifies a dual cdc7/CDK9 inhibitor to sensitise triple-negative breast cancer to EGFR-targeted therapy. *Breast Cancer Res*. 2019;21(1):77.
18. Wang X, Yu C, Wang C, et al. Novel cyclin-dependent kinase 9 (CDK9) inhibitor with suppression of cancer stemness activity against non-small-cell lung cancer. *Eur J Med Chem*. 2019;181: 111535.
19. Zhang H, Pandey S, Travers M, et al. Targeting CDK9 reactivates epigenetically silenced genes in cancer. *Cell*. 2018; 175(5):1244—1258.
20. Ji X, Lu H, Zhou Q, Luo K. LARP7 suppresses P-TEFb activity to inhibit breast cancer progression and metastasis. *Elife*. 2014;3: 02907.
21. Chao J, Cheng HY, Chang ML, et al. Gallic acid ameliorated impaired lipid homeostasis in a mouse model of high-fat diet- and streptozotocin-induced NAFLD and diabetes through improvement of β-oxidation and ketogenesis. *Front Pharmacol*. 2021;11:606759.
22. Liu LJ, Leung KH, Chan DS, Wang YT, Ma DL, Leung CH. Identification of a natural product-like STAT3 dimerization inhibitor by structure-based virtual screening. *Cell Death Dis*. 2014;5(6): 1293.
23. Yang GJ, Ko CN, Zhong HJ, Leung CH, Ma DL. Structure-based discovery of a selective KDM5A inhibitor that exhibits anti-cancer activity via inducing cell cycle arrest and senescence in breast cancer cell lines. *Cancers (Basel)*. 2019;11(1):92.
24. Dai C, Liu MP, Zhang WJ, et al. A material-basis study of Aloe vera on the wnt/β-catenin signaling pathway using a knock-in/knockout method with high-speed countercurrent chromatography. *RSC Adv*. 2017;7:38819—38829.
25. Minzel W, Venkatachalam A, Fink A, et al. Small molecules co-targeting CKIα and the transcriptional kinases CDK7/9 control AML in preclinical models. *Cell*. 2018;175(1):171—185.
26. Zhang GN, Zhang YK, Wang YJ, et al. Modulating the function of ATP-binding cassette subfamily G member 2 (ABCG2) with inhibitor cabozantinib. *Pharmacol Res*. 2017;119:89—98.
27. Zhong HJ, Lu L, Leung KH, et al. An iridium (iii)-based irreversible protein—protein interaction inhibitor of BRD4 as a potent anticancer agent. *Chem Sci*. 2015;6(10): 5400—5408.
28. Yang GJ, Wang W, Lei PM, Leung CH, Ma DL. A 7-methoxybicoumarin derivative selectively inhibits BRD4 BD2 for anti-melanoma therapy. *Int J Biol Macromol*. 2020;164: 3204—3220.
29. Sonawane YA, Taylor MA, Napoleon JV, Rana S, Contreras JI, Natarajan A. Cyclin dependent kinase 9 inhibitors for cancer therapy. *J Med Chem*. 2016;59(19):8667—8684.
30. De Falco G, Giordano A. CDK9: from basal transcription to cancer and AIDS. *Cancer Biol Ther*. 2002;1(4):342—347.
31. Morales F, Giordano A. Overview of CDK9 as a target in cancer research. *Cell Cycle*. 2016;15(4):519—527.
32. Di Micco R, Fontanals-Cirera B, Low V, et al. Control of embryonic stem cell identity by BRD4-dependent transcriptional elongation of super-enhancer-associated pluripotency genes. *Cell Rep*. 2014;9(1):234—247.
33. Cichon MA, Nelson CM, Radisky DC. Regulation of epithelial-mesenchymal transition in breast cancer cells by cell contact and adhesion. *Cancer Inform*. 2015;14(Suppl 3):1—13.
34. Kvokačková B, Remšík J, Jolly MK, Souček K. Phenotypic heterogeneity of triple-negative breast cancer mediated by epithelial—mesenchymal plasticity. *Cancers (Basel)*. 2021; 13(9):2188.
35. Chen C, Okita Y, Watanabe Y, et al. Glycoprotein nmb is exposed on the surface of dormant breast cancer cells and induces stem cell-like properties. *Cancer Res*. 2018;78(22): 6424—6435.
36. Tanabe S, Quader S, Cabral H, Ono R. Interplay of EMT and CSC in cancer and the potential therapeutic strategies. *Front Pharmacol*. 2020;11:904.
37. Sheridan C, Kishimoto H, Fuchs RK, et al. CD44+/CD24- breast cancer cells exhibit enhanced invasive properties: an early step necessary for metastasis. *Breast Cancer Res*. 2006;8(5): R59.
38. He S, Fang X, Xia X, Hou T, Zhang T. Targeting CDK9: a novel biomarker in the treatment of endometrial cancer. *Oncol Rep*. 2020;44(5):1929—1938.
39. Wang J, Dean DC, Hornicek FJ, Shi H, Duan Z. Cyclin-dependent kinase 9 (CDK9) is a novel prognostic marker and therapeutic target in ovarian cancer. *FASEB J*. 2019;33(5): 5990—6000.
40. Sedlacek HH. Mechanisms of action of flavopiridol. *Crit Rev Oncol Hematol*. 2001;38(2):139—170.
41. Shiozaki Y, Okamura K, Kohno S, et al. The CDK9—cyclin T1 complex mediates saturated fatty acid—induced vascular calcification by inducing expression of the transcription factor CHOP. *J Biol Chem*. 2018;293(44):17008—17020.
42. Bhullar KS, Lagarón NO, McGowan EM, et al. Kinase-targeted cancer therapies: progress, challenges and future directions. *Mol Cancer*. 2018;17(1):48.

43. Krystof V, Baumli S, Fürst R. Perspective of cyclin-dependent kinase 9 (CDK9) as a drug target. *Curr Pharm Des*. 2012; 18(20):2883—2890.
44. Cheng SS, Yang GJ, Wang W, Leung CH, Ma DL. The design and development of covalent protein-protein interaction inhibitors for cancer treatment. *J Hematol Oncol*. 2020;13(1):26.
45. Randjelović J, Erić S, Savić V. Computational study and peptide inhibitors design for the CDK9—cyclin T1 complex. *J Mol Model*. 2013;19(4):1711—1725.
46. Randjelovic J, Eric S, Savic V. In silico design of small molecule inhibitors of CDK9/cyclin T1 interaction. *J Mol Graph Model*. 2014;50:100—112.
47. Hussain A, Verma CK, Chouhan U. Identification of novel inhibitors against Cyclin Dependent Kinase 9/Cyclin T1 complex as: anti cancer agent. *Saudi J Biol Sci*. 2017;24(6):1229—1242.
48. Zhong HJ, Liu LJ, Chong CM, et al. Discovery of a natural product-like iNOS inhibitor by molecular docking with potential neuroprotective effects in vivo. *PLoS One*. 2014;9(4): 92905.
49. Polier G, Ding J, Konkimalla BV, et al. Wogonin and related natural flavones are inhibitors of CDK9 that induce apoptosis in cancer cells by transcriptional suppression of Mcl-1. *Cell Death Dis*. 2011;2(7):e182.
50. Zimmermann TJ, Roy S, Martinez NE, Ziegler S, Hedberg C, Waldmann H. Biology-oriented synthesis of a tetrahydroisoquinoline-based compound collection targeting microtubule polymerization. *Chembiochem*. 2013;14(3): 295—300.
51. Leroux AE, Biondi RM. Renaissance of allostery to disrupt protein kinase interactions. *Trends Biochem Sci*. 2020;45(1): 27—41.
52. Leonard SE, Register AC, Krishnamurty R, Brighty GJ, Maly DJ. Divergent modulation of Src-family kinase regulatory interactions with ATP-competitive inhibitors. *ACS Chem Biol*. 2014;9(8):1894—1905.
53. Polier S, Samant RS, Clarke PA, Workman P, Prodromou C, Pearl LH. ATP-competitive inhibitors block protein kinase recruitment to the Hsp90-Cdc37 system. *Nat Chem Biol*. 2013; 9(5):307—312.
54. Shao H, Zhu Q, Lu H, et al. HEXIM1 controls P-TEFb processing and regulates drug sensitivity in triple—negative breast cancer. *Mol Biol Cell*. 2020;31(17):1867—1878.
55. Zhou JM, Hu SQ, Jiang H, et al. OCT4B1 promoted EMT and regulated the self-renewal of CSCs in CRC: effects associated with the balance of miR-8064/PLK1. *Mol Ther Oncolytics*. 2019; 15:7—20.